Nonreciprocal phonon laser in a spinning microwave magnomechanical system

Yi Xu,[1] Jin-Yu Liu,[1] Wenjing Liu,[1,*] and Yun-Feng Xiao[1,2,3]

[1]*State Key Laboratory for Mesoscopic Physics and Frontiers Science Center for Nano-ptoelectronics, School of Physics, Peking University, 100871 Beijing, China*
[2]*Collaborative Innovation Center of Extreme Optics, Shanxi University, 030006 Taiyuan, China*
[3]*Peking University Yangtze Delta Institute of Optoelectronics, Nantong, 226010 Jiangsu, China*

A nonreciprocal phonon laser in a spinning microwave magnomechanical system is proposed. The system consists of a spinning microwave resonator coupled with an yttrium iron garnet sphere. The Fizeau light-dragging effect caused by the spinning of the resonator leads to a significant difference in the mechanical gain and the threshold power for driving the resonator from the opposite directions, which results in a nonreciprocal phonon laser. The nonreciprocal phonon laser is highly tunable by the spinning speed and direction of the resonator. These results provide an experimentally feasible approach for exploring various nonreciprocal effects in cavity magnomechanical systems, and may find applications in photon, magnon, and phonon manipulations in many-body coupled systems.

I. INTRODUCTION

Since the realization of the first laser by Maiman in 1960 [1], lasers have spawned the emergence of various new research areas and the discovery of miscellaneous new physical phenomena. Inspired by optical lasers, many researchers have drawn their attentions to phonon lasers (i.e., phonon amplification by stimulated emission) due to the similarity between the bosonic photons and phonons. As early as in 2003, Chen and Khurgin proposed the possibility of realizing phonon lasers in a practical scheme [2]. Soon after, phonon lasers have been experimentally achieved in single trapped ions [3], semiconductor superlattices [4], and cavity optomechanical systems [5]. Phonon lasers provide an important platform for quantum acoustics [6,7], functional phononic devices [8,9], and nondestructive precision measurements or imaging [10–12].

Nonreciprocal transmission and amplification of phonons are of great interest in energy and mechanical engineering [13–18], such as phononic diodes, acoustic sensing, and phonon-based information processing. Recently, by coupling an optomechanical resonator with a spinning optical resonator, a nonreciprocal phonon laser was theoretically proposed [19]. However, the proposed scheme is technically challenging, as it requires spinning the optical resonator while maintaining a stable inter-cavity coupling strength. Thus, nonreciprocal phonon laser designs with improved experimental feasibility are highly desired.

Spinning magnomechanical microcavities may provide a promising alternative. Yttrium iron garnet (YIG) is one of the widely adopted ferrimagnetic materials in magnomechanical systems due to its high spin density and low damping rate

[20]. Strong and even ultrastrong coupling between the Kittel mode [21] (the ferromagnetic mode) in a YIG sphere and the microwave cavity photons have been experimentally achieved [20,22–27], which results in cavity-magnon polaritons. Besides, a YIG sphere can also serve as an excellent mechanical resonator [28], in which magnon and phonon modes are coupled via a nonlinear magnetostrictive interaction. In contrast to the radiation force [29–32], electrostatic force [33,34], and piezoelectric force [35] used for the photon-phonon coupling in cavity opto- and electromechanical systems, such a radiation-pressure-like magnetiostrictive force is highly tunable via external magnetic fields, providing new opportunities to achieve actively controllable hybrid quantum systems [28]. Recently, nonreciprocal transmission and entanglement in magnomechanical systems have been theoretically proposed [36] by exploiting the Fizeau light-dragging effect [37,38].

The proposed nonreciprocal phonon laser is composed of a spinning microwave magnomechanical system with a YIG sphere placed inside. Such a spinning resonator device with whispering gallery modes (WGMs) has already proved to be experimentally accessible [37]. The phonon lasing can be enhanced for driving the system from one direction and suppressed for driving from the opposite direction. This nonreciprocity originates from the Fizeau light-dragging effect by spinning the microcavity, which modulates both the mechanical gain and threshold power. Therefore, a highly tunable nonreciprocal phonon laser can be achieved by adjusting the spinning speed and direction of the resonantor.

II. THEORETICAL MODEL

A schematic of the cavity magnomechanical system is shown in Fig. 1(a). It consists of a microwave resonator with resonance frequency ω_a and a YIG sphere placed inside near the maximum magnetic field of the system. The WGM
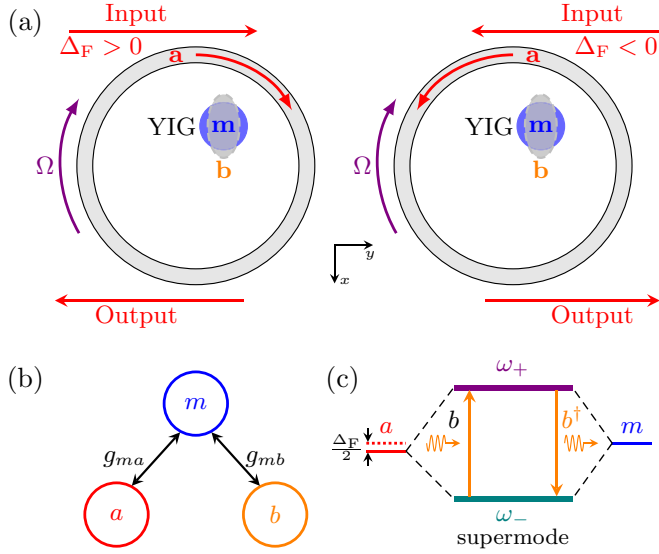
*wenjingl@pku.edu.cn

FIG. 1. (a) Schematic of the system. Driving the resonator from the left (y axis) results in a Fizeau shift $\Delta_F > 0$, while $\Delta_F < 0$ for driving from the right ($-y$ axis). (b) Interactions among the subsystems. (c) The equivalent two-level phonon laser energy-level diagram.

geometry that support two counterpropagating modes is critical to introduce the Fizeau shift and noneciprocity. The YIG sphere supports both the magnon and phonon modes [28]. By spinning the resonator along the clockwise direction, the microwave circulating in the resonator undergoes a Fizeau shift [37]

$$\Delta_F = \pm \Omega \frac{nr\omega_a}{c} \left(1 - \frac{1}{n^2} - \frac{\lambda}{n} \frac{dn}{d\lambda} \right). \quad (1)$$

Here, Ω is the angular velocity of the spinning resonantor; n and r are the refractive index and radius of the resonator, respectively. c and λ are the speed of the light and the wavelength of the microwave photon in vacuum, respectively. The dispersion term $(\lambda/n)(dn/d\lambda)$ is typically small and thus negligible [19,37]. $\Delta_F > 0$ denotes driving the resonator from the left, corresponding to the situation in which the resonator spinning and microwave rotation are along the same direction [see Fig. 1(a)]. In contrast, driving the resonator from the right results in $\Delta_F < 0$, where the resonator spinning and microwave rotation are in opposite directions.

The Hamiltonian of the system in the frame rotating at the cavity drive frequency ω_d can be written as

$$H = \hbar(-\Delta_a - \Delta_F)a^\dagger a - \hbar\Delta_m m^\dagger m + \hbar\omega_b b^\dagger b$$
$$+ \hbar g_{ma}(m^\dagger a + a^\dagger m) + \hbar g_{mb} m^\dagger m(b + b^\dagger)$$
$$+ i\hbar\varepsilon_d(a^\dagger - a) \quad (2)$$

with the rotating-wave approximation (see Appendix A). Here, a ($a^\dagger$) and b ($b^\dagger$) are the annihilation (creation) operators of the cavity photon and phonon modes, respectively. The annihilation and creation operators of the magnon mode are denoted as m and $m^\dagger$, respectively. ω_b and ω_m represent the resonance frequencies of phonon and magnon modes, respectively. $\Delta_a = \omega_d - \omega_a$ ($\Delta_m = \omega_d - \omega_m$) is the detuning between the driving field and the photon (magnon) mode.

The first term of the Hamiltonian in Eq. (2) describes the cavity photon mode in the spinning resonator, while the second and third terms describe the phonon and magnon modes, respectively. The fourth (fifth) term denotes the coupling between photon (phonon) and magnon modes with the coupling strength g_{ma} (g_{mb}). In contrast to the linear magnon-photon coupling, the magnon and phonon modes are coupled via a nonlinear magnetostrictive interaction. A microwave driving field with the amplitude $\varepsilon_d = \sqrt{2\kappa_a P_{in}/\hbar\omega_d}$ is applied to the resonator, and is described by the last term in Eq. (2). Here, κ_a is the decay rate of the cavity mode, and P_{in} is the input power of the driving field.

The steady-state solutions of the system can be obtained as (see Appendix A)

$$b_s = \frac{ig_{mb}|m_s|^2}{-i\omega_b - \kappa_b},$$

$$a_s = \frac{ig_{ma}m_s - \varepsilon_d}{i\Delta_a + i\Delta_F - \kappa_a},$$

$$m_s = \frac{ig_{ma}a_s}{(i\Delta_m - \kappa_m) - ig_{mb}(b_s + b_s^*)}. \quad (3)$$

Here, κ_b is the dissipation rate of the mechanical mode, and κ_m is the decay rate of the magnon mode. The steady-state mechanical displacement x_s is proportional to

$$b_s + b_s^* = \frac{i\Delta_m - \kappa_m}{ig_{mb}} + \frac{g_{ma}(\varepsilon_d - ig_{ma}m_s)}{g_{mb}m_s(i\Delta_a + i\Delta_F - \kappa_a)}, \quad (4)$$

which clearly depends on the Fizeau shift Δ_F. A mechanical displacement amplification factor $\eta_{>,<}$ is defined to describe the enhanced steady-state mechanical displacement of the spinning resonator compared to the static resonator,

$$\eta_{>,<} = \frac{x_s(\Delta_F > 0, < 0)}{x_s(\Delta_F = 0)}. \quad (5)$$

Using the supermode operators $\Psi_\pm = (a \pm m)/\sqrt{2}$, the Hamiltonian of the system can be rewritten as

$$H = \hbar\omega_+ \Psi_+^\dagger \Psi_+ + \hbar\omega_- \Psi_-^\dagger \Psi_- + \hbar\omega_b b^\dagger b$$
$$- \frac{\hbar g_{mb}}{2}(\Psi_+^\dagger \Psi_- b + b^\dagger \Psi_-^\dagger \Psi_+)$$
$$+ \frac{\hbar}{2}(\Psi_+^\dagger \Psi_- + \Psi_-^\dagger \Psi_+)(\Delta_m - \Delta_a - \Delta_F)$$
$$+ i\frac{\hbar\varepsilon_d}{\sqrt{2}}[(\Psi_+^\dagger + \Psi_-^\dagger) - (\Psi_+ + \Psi_-)] \quad (6)$$

after applying the rotating-wave approximation. The first and second terms describe the Hamiltonian of the supermodes Ψ_+ and Ψ_- with the frequencies $\omega_+ = -(\Delta_a + \Delta_m + \Delta_F)/2 + g_{ma}$ and $\omega_- = -(\Delta_a + \Delta_m + \Delta_F)/2 - g_{ma}$, respectively. The third term describes the absorption and emission of phonons between two nondegenerate supermodes $\Psi_\pm$. The interaction of the system thus can be understood by the energy diagram in Fig. 1(c), analogous to a photon laser based on two-level atomic ensembles [39,40]. The fourth term adds a nonreciprocal detuning between the magnon and the cavity photon, which modifies the supermode energies and thus the phonon lasing process [5,19,41]. The last term denotes the interactions

between the driving field and the two nondegenerate supermodes $\Psi_{\pm}$.

The mechanical gain G can be obtained from the Hamiltonian in Eq. (6) (see Appendix B):

$$G = \frac{g_{mb}^2 \gamma \, \delta n / \kappa_b}{8\gamma^2 + 2(2g_{ma} - \omega_b)^2}$$
$$- \frac{g_{mb}^2 \varepsilon_d^2 \gamma (\Delta_m + \Delta_a + \Delta_{\mathrm{F}})(2g_{ma} - \omega_b)/\kappa_b}{[16\gamma^2 + 4(2g_{ma} - \omega_b)^2][\beta^2 + \gamma^2(\Delta_m + \Delta_a + \Delta_{\mathrm{F}})^2]}.$$
$$(7)$$

Here, $\gamma = (\kappa_a + \kappa_m)/2$, and $\delta n = \Psi_+^\dagger \Psi_+ - \Psi_-^\dagger \Psi_-$ is the population difference between the supermodes Ψ_+ and Ψ_-. $\beta = \beta_0 - \Delta_m \Delta_{\mathrm{F}} - g_{mb}(\Delta_m - \Delta_a - \Delta_{\mathrm{F}}) \operatorname{Re}[b]/2$, $\beta_0 = g_{ma}^2 + \gamma^2 - \Delta_m \Delta_a + g_{mb}^2 n_b/4$, and $n_b = b^\dagger b$ is the phonon number.

The first term of the mechanical gain G is proportional to the population inversion δn, while the second term originates from the driving terms for the unpaired supermode operators in Eq. (B1) [39]. Note that both δn and the second term of G depend on Δ_{F}, which is quite different from the conventional phonon laser system without spinning components [5,39,41]. Thus, different mechanical gains G can be obtained for the $\Delta_{\mathrm{F}} > 0$ and $\Delta_{\mathrm{F}} < 0$ cases, which makes it possible to achieve a nonreciprocal phonon laser. With the mechanical gain $G > 1$, the phonon mode can be amplified [see Eq. (B4)]. The threshold condition for phonon lasing is $G = 1$, and the stimulated emitted phonon number is

$$N_b = \exp[2(G-1)]. \tag{8}$$

The corresponding threshold pump power P_{th} can be evaluated with the threshold condition and Eq. (7).

III. RESULTS AND DISCUSSION

The supermode operators are generally adopted for the coupled degenerate resonators [5,19,39,41–43]. Here, the magnon and photon modes are assumed to be in resonance, that is $\Delta_a = \Delta_m = \Delta$. The steady-state populations of photon and magnon modes are investigated as a function of the normalized detuning Δ/ω_b, as shown in Figs. 2(a) and 2(b), respectively. It is found that different driving directions (the left or right) result in different steady-state magnon numbers $|m_s|^2$ and photon numbers $|a_s|^2$. Compared with the stationary magnomechanical system (i.e., no spinning with $\Delta_{\mathrm{F}} = 0$), the magnon number $|m_s|^2$ (photon number $|a_s|^2$) of the spinning magnomechanical system increases (decreases) for $\Delta_{\mathrm{F}} > 0$, while it decreases (increases) for $\Delta_{\mathrm{F}} < 0$. This variations of magnon number then modifies the magnetostrictive force (radiation-pressure-like). Therefore, the magnon-phonon coupling strength can be tuned by the driving direction (or the spinning direction) and the spinning speed of the resonator. As a result, the steady-state mechanical displacement x_s of the spinning magnomechanical system can be enhanced (i.e., $\eta_{>,<} > 1$), as shown in Fig. 2(c). This indicates the enhancement of photon generation in the spinning system.

In Fig. 3(a), the mechanical gain G is plotted as the function of the normalized detuning Δ/ω_b and the magnon-photon coupling strength g_{ma} for $\Delta_{\mathrm{F}} < 0$. The mechanical gain $G > 1$ is available with the proper selection of Δ_a and g_{ma}, making
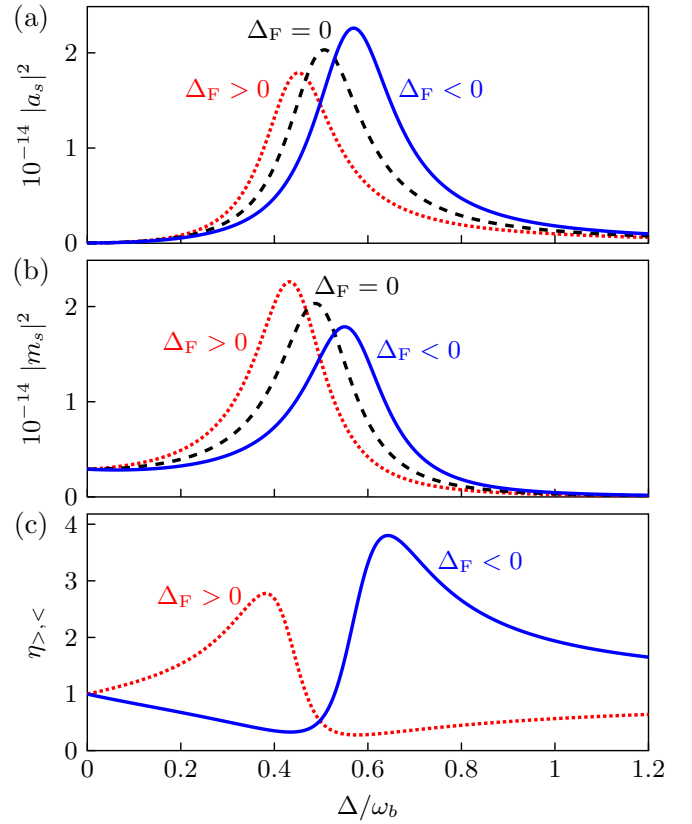

FIG. 2. The (a) steady-state photon number $|a_s|^2$, (b) steady-state magnon number $|m_s|^2$, and (c) mechanical amplification factor $\eta_{>,<}$ as a function of the normalized detuning Δ/ω_b. Here, a set of experimentally feasible values are used [28]: $\omega_b/2\pi = 11.42$ MHz, $g_{ma} = 0.5\omega_b$, $g_{mb}/2\pi = 4.1$ mHz, $2\kappa_a/2\pi = 3.35$ MHz, $2\kappa_m/2\pi = 1.12$ MHz, $2\kappa_b/2\pi = 300$ Hz, $P_{\mathrm{in}} = 10$ mW, and $\omega_d/2\pi = 8$ GHz. The Fizeau shift is $|\Delta_{\mathrm{F}}| = 0.12\omega_b$.

phonon lasing possible. A maximum mechanical gain $G \approx 5.6$ is obtained with $g_{ma}/\omega_b = 0.49$ and $\Delta/\omega_b = 0.55$. Specifically, the mechanical gain G as a function of the normalized detuning Δ/ω_b with $g_{ma}/\omega_b = 0.49$ is shown in Fig. 3(b). For the stationary magnomechanical system ($\Delta_{\mathrm{F}} = 0$), the mechanical gain G is always the same no matter whether the resonator is driven from the left or right. The maximum G is located at $\Delta/\omega_b \approx 0.5$, as shown in Fig. 3(b). By spinning the resonator, the peak position of the mechanical gain moves towards the left (right) with $\Delta_{\mathrm{F}} > 0$ ($\Delta_{\mathrm{F}} < 0$). Then by adjusting the detuning Δ, we can get enhanced mechanical gain for driving the resonator from one direction and suppressed mechanical gain for driving from the opposite direction. For example, within the normalized detuning Δ/ω_b in the range from 0.68 to 0.76, the mechanical gain G is enhanced for the $\Delta_{\mathrm{F}} < 0$ case, while it is suppressed for the $\Delta_{\mathrm{F}} > 0$ case. This spinning-induced direction-dependent mechanical gain can be attributed to the nonreciprocal microwave transmission, which was theoretically investigated in a recent work [36]. This nonreciprocal microwave transmission results in different magnetostrictive forces for driving the resonator in opposite directions, which in turn shows enhanced or suppressed mechanical gain for different driving directions.
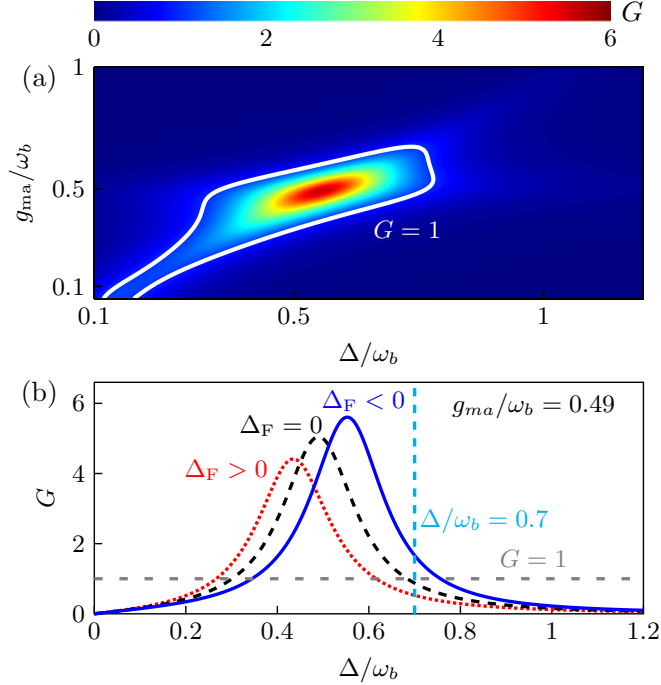
FIG. 3. (a) The mechanical gain G versus the normalized detuning Δ/ω_b and the magnon-photon coupling strength g_{ma} for the $\Delta_F < 0$ case. The white curve corresponds to $G = 1$. (b) The mechanical gain G as a function of the normalized detuning Δ/ω_b with $g_{ma}/\omega_b = 0.49$. The other parameters are the same as those in Fig. 2.

FIG. 4. (a) The stimulated emitted phonon number N_b as a function of the pump power P_{in} with the Fizeau shift $|\Delta_F|/\omega_b = 0.12$. The threshold power P_{th} denoted by the thick point is obtained from the threshold condition. (b) The threshold power P_{th} as a function of the Fizeau shift $|\Delta_F|$. Here, $g_{ma}/\omega_b = 0.49$ and $\Delta/\omega_b = 0.7$. The other parameters are the same as those in Fig. 2.

With the enhanced mechanical gain $G > 1$, the phonon mode can be amplified. The stimulated emitted phonon number N_b as a function of the pump power P_{in} with $g_{ma}/\omega_b = 0.49$ and $\Delta/\omega_b = 0.7$ is shown in Fig. 4(a). The choice of $\Delta/\omega_b = 0.7$ gives $G > 1$ for the $\Delta_F < 0$ case and $G < 1$ for the $\Delta_F > 0$ case. It is clearly seen that the Fizeau shift has a significant impact on the threshold power P_{th}. For the stationary case ($\Delta_F = 0$), the threshold power is about 11.44 mW. The threshold power is then reduced to 5.99 mW by spinning the resonator with $\Delta_F < 0$, which is attributed to the enhanced mechanical gain [see Fig. 3(b)]. In contrast, the mechanical gain for the $\Delta_F > 0$ case is suppressed, and a larger pump power ($\sim$18.98 mW) is required to realize the phonon lasing. In addition, the threshold power P_{th} can be further reduced to 1.75 mW when the maximum mechanical gain is achieved at $\Delta/\omega_b = 0.55$ for the $\Delta_F < 0$ case [see Fig. 3(b)].

The Fizeau shift Δ_F can be easily tuned by adjusting the spinning speed Ω [see Eq. (1)]. The effect of the Fizeau shift Δ_F on the threshold power P_{th} is shown in Fig. 4(b). The threshold power P_{th} decreases with $|\Delta_F|$ for the $\Delta_F < 0$ case and increases for the $\Delta_F > 0$ case. Therefore, lower threshold power P_{th} is needed for the $\Delta_F < 0$ case, compared with the stationary resonator case ($\Delta_F = 0$). For example, the threshold power is $P_{th} = 4.98$ mW with $\Delta_F/\omega_b = -0.15$. In contrast, more than two times input power ($P_{th} = 11.43$ mW) is required for the stationary resonator case. For the $\Delta_F > 0$ case, much higher threshold power ($P_{th} = 21.2$ mW) is needed to achieve the phonon lasing due to the suppressed mechanical gain at $\Delta/\omega_b = 0.7$.
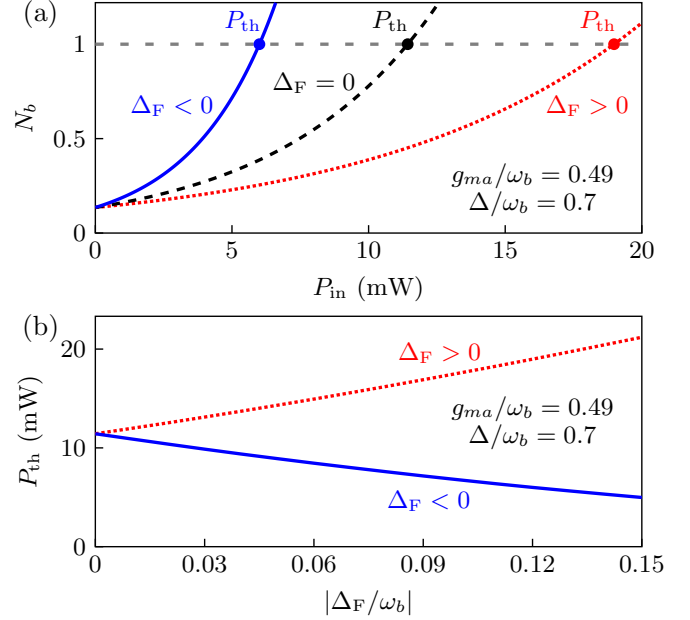
To clearly see the effect of spinning on the nonreciprocal phonon laser, an isolation parameter

$$\Re = 10 \log_{10} \frac{N_b(\Delta_F < 0)}{N_b(\Delta_F > 0)} \tag{9}$$

is introduced. For a phonon laser without the spinning resonator (i.e., a conventional reciprocal phonon laser), the isolation parameter is $\Re = 0$. A nonzero $\Re$ indicates the emergence of nonreciprocity in the phonon lasing action. The isolation parameter $\Re$ as the function of the Fizeau shift $|\Delta_F|$ and the normalized detuning Δ/ω_b is shown in Fig. 5, in which only the phonon lasing regime (i.e., $N_b \geqslant 1$) is pre-
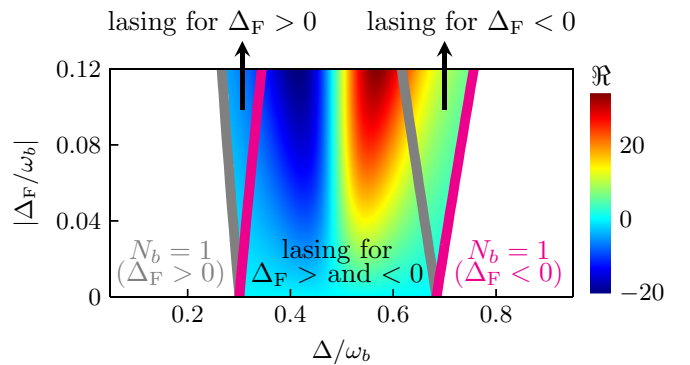

FIG. 5. The isolation parameter $\Re$ versus the Fizeau shift $|\Delta_F|$ and normalized detuning Δ/ω_b. The black and magenta curves correspond to $N_b = 1$ for the $\Delta_F > 0$ and $\Delta_F < 0$ cases, respectively. The white regions denote $N_b < 1$. Here, $g_{ma}/\omega_b = 0.49$, and the other parameters are the same as those in Fig. 2.
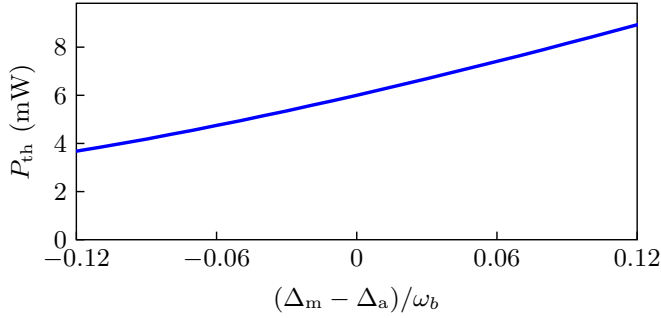
FIG. 6. The threshold power P_{th} as a function of the normalized detuning difference between magnon and photon modes $(\Delta_m - \Delta_a)/\omega_b$. Here, $\Delta_F/\omega_b = -0.12$, $g_{ma}/\omega_b = 0.49$, and $\Delta_a/\omega_b = 0.7$. The other parameters are the same as those in Fig. 2.

sented. A nonreciprocal phonon laser can be obtained by adjusting the normalized detuning, and the maximum isolation rate $\Re \sim 34$ dB can be achieved. In addition, the regimes where phonon lasing only occurs for one driving direction but not the opposite can easily be found in Fig. 5. Therefore, phonon lasing can be readily switched on and off by adjusting the driving direction or the spinning direction of the resonator.

The magnon-photon coupling strength g_{ma} depends on the cavity mode volume, magnetic dipole moment, and the position of YIG sphere in the resonator, which may vary in different cavity designs. However, we should note that, the nonreciprocity is insensitive to the absolute value of g_{ma}. Although a smaller g_{ma} results in smaller mechanical gain and higher threshold power for the system, a nonreciprocal phonon laser can still be achieved (see Fig. 7). In an experi-
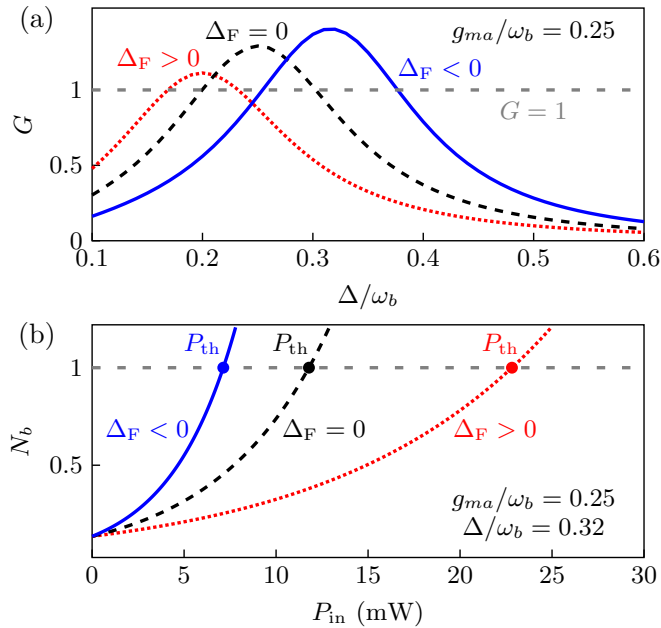

FIG. 7. (a) The mechanical gain G as a function of the normalized detuning Δ/ω_b. (b) The stimulated emitted phonon number N_b as a function of the pump power P_{in} with the Fizeau shift $|\Delta_F|/\omega_b = 0.12$. The threshold power P_{th} denoted by the thick point is obtained from the threshold condition. Here, $g_{ma}/\omega_b = 0.25$ and $\Delta/\omega_b = 0.32$. The other parameters are the same as those in Fig. 2.
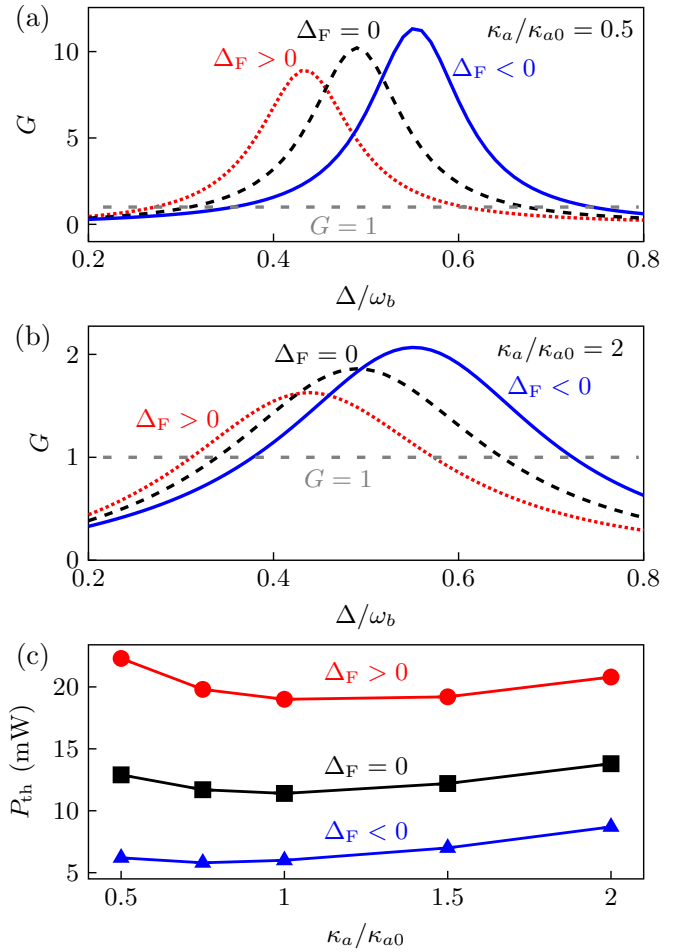

FIG. 8. The mechanical gain G as a function of the normalized detuning Δ/ω_b with (a) $\kappa_a/\kappa_{a0} = 0.5$, and (b) $\kappa_a/\kappa_{a0} = 2$. (c) The threshold power P_{th} as a function of the normalized decay rate of photon mode κ_a/κ_{a0} with $\Delta/\omega_b = 0.7$. Here, $2\kappa_{a0}/2\pi = 3.35$ MHz, $g_{ma}/\omega_b = 0.49$, and the other parameters are the same as those in Fig. 2.

ment, the decay rate of the photon mode κ_a can be engineered, while the decay rate of magnon mode κ_m is given by the material system. The effect of κ_a and κ_m on the mechanical gain and threshold power are shown in Figs. 8 and 9, respectively. It is found that a larger mechanical gain can be achieved with smaller κ_a (κ_m). The nonreciprocity in the phonon lasing action can still be obtained with smaller or larger κ_a (κ_m). The nonreciprocity is introduced by the Fizeau shift, which is proportional to the radius and the spinning speed of the resonator. For example, in a microwave resonator with radius of 6 cm and the relative permittivity of 80 [44], a spinning speed of 12.9 kHz gives rise to the Fizeau shift of $0.1\omega_b$. As a much smaller Fizeau shift (e.g., $0.03\omega_b$) can already introduce a pronounced nonreciprocity sufficient for phonon laser applications [see Fig. 4(b)], the spinning speed required in this proposal is experimentally feasible [37].

The magnon and photon modes are assumed have the same frequencies (i.e., $\Delta_a = \Delta_m = \Delta$) in the studies above. Noted that the magnon frequency is tunable with the external bias magnetic field [20,28]. Thus the threshold power P_{th} can be
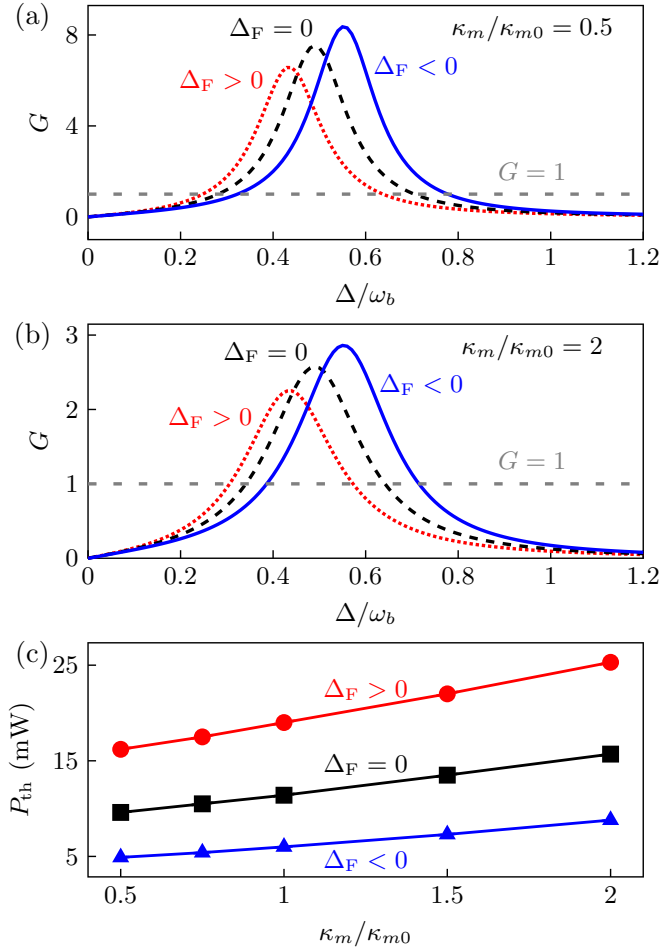
FIG. 9. The mechanical gain G as a function of the normalized detuning Δ/ω_b with (a) $\kappa_m/\kappa_{m0} = 0.5$ and (b) $\kappa_m/\kappa_{m0} = 2$. (c) The threshold power P_{th} as a function of the normalized decay rate of magnon mode κ_m/κ_{m0} with $\Delta/\omega_b = 0.7$. Here, $2\kappa_{m0}/2\pi = 1.12$ MHz, $g_{ma}/\omega_b = 0.49$, and the other parameters are the same as those in Fig. 2.

further tuned by controlling the external bias magnetic field (i.e., the magnon mode detuning Δ_m), as shown in Fig. 6. For the $\Delta_F < 0$ case, the threshold power P_{th} is reduced to ~ 3.68 mW with $\Delta_m = \Delta_a + \Delta_F$.

IV. CONCLUSION

In summary, we have studied a nonreciprocal phonon laser in a spinning microwave magnomechanical system. By spinning the microwave resonator, the Fizeau light-dragging effect is introduced into the system, which significantly modifies the steady-state magnon number, photon number, and the steady-state mechanical displacement. The mechanical gain for phonon lasing in the spinning microwave magnomechanical system depends on the driving direction, making it possible to achieve a nonreciprocal phonon laser. The mechanical gain and the threshold power can be actively modulated by adjusting the spinning speed, spinning direction or external bias magnetic field. These results provide a different route for manipulating cavity magnomechanical systems

through the Fizeau light-dragging effect, and may lead to applications in various acoustic devices.

APPENDIX A: SYSTEM HAMILTONIAN AND THE STEADY-STATE SOLUTIONS

The Hamiltonian of the investigated system can be written as

$$H = \hbar(\omega_a - \Delta_F)a^\dagger a + \hbar\omega_b b^\dagger b + \hbar\omega_m m^\dagger m$$
$$+ \hbar g_{ma}(a + a^\dagger)(m + m^\dagger) + \hbar g_{mb}m^\dagger m(b + b^\dagger)$$
$$+ i\hbar\varepsilon_d(a^\dagger e^{-i\omega_d t} - a e^{i\omega_d t}). \tag{A1}$$

Here, the first term describes the cavity photon mode in the spinning resonator, while the second and third terms describe the phonon and magnon modes, respectively. The fourth term denotes the coupling between photon and magnon modes with the coupling strength g_{ma}. The phonon-magnon interaction with the coupling strength g_{mb} arising from the magnetostrictive interaction is described by the fifth term. The last term describes the interaction between the microwave driving field and the resonator.

In the frame rotating at the cavity drive frequency ω_d, the Hamiltonian in Eq. (A1) is given as

$$H = \hbar(-\Delta_a - \Delta_F)a^\dagger a - \hbar\Delta_m m^\dagger m + \hbar\omega_b b^\dagger b$$
$$+ \hbar g_{ma}(m^\dagger a + a^\dagger m) + \hbar g_{mb}m^\dagger m(b + b^\dagger)$$
$$+ i\hbar\varepsilon_d(a^\dagger - a) \tag{A2}$$

with $\Delta_a = \omega_d - \omega_a$ and $\Delta_m = \omega_d - \omega_m$. Here, the rotating-wave approximation is adopted, in which the term $g_{ma}(a + a^\dagger)(m + m^\dagger)$ changes to $g_{ma}(am^\dagger + a^\dagger m)$. This approximation is valid for $\omega_a, \omega_m \gg g_{ma}, \kappa_a, \kappa_m$.

The quantum Langevin equations of the system are then given as

$$\dot{a} = (i\Delta_a + i\Delta_F - \kappa_a)a - ig_{ma}m + \varepsilon_d + \sqrt{2\kappa_a}a_{in},$$
$$\dot{m} = (i\Delta_m - \kappa_m)m - ig_{ma}a - ig_{mb}m(b + b^\dagger)$$
$$+ \sqrt{2\kappa_m}m_{in},$$
$$\dot{b} = -(i\omega_b + \kappa_b)b - ig_{mb}m^\dagger m + \sqrt{2\kappa_b}b_{in}. \tag{A3}$$

Here, a_{in}, m_{in}, and b_{in} are the input noise operators affecting the photon, magnon, and mechanical modes, respectively. With strong driving conditions, the quantum noise terms in Eq. (A3) can be safely ignored since only the mean-number behaviors are interested in this work [5,19,41]. The steady-state solutions of the system can be obtained as

$$b_s = \frac{ig_{mb}|m_s|^2}{-i\omega_b - \kappa_b}, \quad a_s = \frac{ig_{ma}m_s - \varepsilon_d}{i\Delta_a + i\Delta_F - \kappa_a},$$

$$m_s = \frac{ig_{ma}a_s}{(i\Delta_m - \kappa_m) - ig_{mb}(b_s + b_s^*)}. \tag{A4}$$

APPENDIX B: MECHANICAL GAIN

The dynamical equations for the supermodes $\Psi_\pm$ and phonon mode b can be obtained from Eq. (6):

$$
\begin{aligned}
\dot{\Psi}_+ &= -(i\omega_+ + \gamma)\Psi_+ + ig_{mb}\Psi_- b/2 \\
&\quad - i(\Delta_m - \Delta_a - \Delta_F)\Psi_-/2 + \varepsilon_d/\sqrt{2}, \\
\dot{\Psi}_- &= -(i\omega_- + \gamma)\Psi_- + ig_{mb}b^\dagger\Psi_+/2 \\
&\quad - i(\Delta_m - \Delta_a - \Delta_F)\Psi_+/2 + \varepsilon_d/\sqrt{2}, \\
\dot{b} &= -(i\omega_b + \kappa_b)b + ig_{mb}\Psi_-^\dagger\Psi_+/2, \quad (B1)
\end{aligned}
$$

where $\gamma = (\kappa_a + \kappa_m)/2$.

The above dynamical equations can be rewritten as

$$
\begin{aligned}
\dot{b} &= -(i\omega_b + \kappa_b)b + ig_{mb}p/2, \\
\dot{p} &= -2(ig_{ma} + \gamma)p + i(\Delta_m - \Delta_a - \Delta_F - g_{mb}b)\delta n/2 \\
&\quad + (\Psi_+ + \Psi_-^\dagger)\varepsilon_d/\sqrt{2}, \quad (B2)
\end{aligned}
$$

with the definition of the ladder operator $p = \Psi_-^\dagger\Psi_+$. $\delta n = \Psi_+^\dagger\Psi_+ - \Psi_-^\dagger\Psi_-$ is the population difference between the supermodes Ψ_+ and Ψ_-.

From Eqs. (B1) and (B2), the steady-state values of $\Psi_\pm$ and p can be obtained as

$$
\begin{aligned}
\Psi_{+,s} &= \frac{\varepsilon_d[2i\omega_- + 2\gamma + ig_{mb}b - i(\Delta_m - \Delta_a - \Delta_F)]}{2\sqrt{2}[\beta - i\gamma(\Delta_m + \Delta_a + \Delta_F)]}, \\
\Psi_{-,s} &= \frac{\varepsilon_d[2i\omega_+ + 2\gamma + ig_{mb}b^\dagger - i(\Delta_m - \Delta_a - \Delta_F)]}{2\sqrt{2}[\beta - i\gamma(\Delta_m + \Delta_a + \Delta_F)]}, \\
p_s &= \frac{i(\Delta_m - \Delta_a - \Delta_F - g_{mb}b)\delta n + \sqrt{2}(\Psi_{+,s} + \Psi_{-,s}^\dagger)\varepsilon_d}{2i(2g_{ma} - \omega_b) + 4\gamma}. \\
&\quad\quad\quad\quad\quad\quad\quad\quad\quad\quad\quad\quad\quad (B3)
\end{aligned}
$$

Here, $\beta = \beta_0 - \Delta_m\Delta_F - g_{mb}(\Delta_m - \Delta_a - \Delta_F)\,\mathrm{Re}[b]/2$, $\beta_0 = g_{ma}^2 + \gamma^2 - \Delta_m\Delta_a + g_{mb}^2 n_b/4$, and $n_b = b^\dagger b$ is the phonon number.

From Eqs. (B2) and (B3), we can get

$$
\dot{b} = (-i\omega_b - i\omega' + G' - \kappa_b)b + D. \quad (B4)
$$

Here,

$$
\begin{aligned}
D &= \frac{-g_{mb}(\Delta_m - \Delta_a - \Delta_F)\delta n}{8\gamma + 4i(2g_{ma} - \omega_b)} \\
&\quad + \frac{ig_{mb}\varepsilon_d^2[\beta(\gamma - ig_{ma}) + \gamma\Delta_m(\Delta_m + \Delta_a + \Delta_F)]}{[4\gamma + 2i(2g_{ma} - \omega_b)][\beta^2 + \gamma^2(\Delta_m + \Delta_a + \Delta_F)^2]}, \\
&\quad\quad\quad\quad\quad\quad\quad\quad\quad\quad\quad\quad\quad\quad (B5)
\end{aligned}
$$

$$
\begin{aligned}
\omega' &= \frac{g_{mb}^2(2g_{ma} - \omega_b)\delta n}{16\gamma^2 + 4(2g_{ma} - \omega_b)^2} \\
&\quad + \frac{g_{mb}^2\varepsilon_d^2\gamma^2(\Delta_m + \Delta_a + \Delta_F)}{[8\gamma^2 + 2(2g_{ma} - \omega_b)^2][\beta^2 + \gamma^2(\Delta_m + \Delta_a + \Delta_F)^2]}, \\
&\quad\quad\quad\quad\quad\quad\quad\quad\quad\quad\quad\quad\quad\quad (B6)
\end{aligned}
$$

and

$$
\begin{aligned}
G' &= \frac{g_{mb}^2\gamma\delta n}{8\gamma^2 + 2(2g_{ma} - \omega_b)^2} \\
&\quad - \frac{g_{mb}^2\varepsilon_d^2\gamma(\Delta_m + \Delta_a + \Delta_F)(2g_{ma} - \omega_b)}{[16\gamma^2 + 4(2g_{ma} - \omega_b)^2][\beta^2 + \gamma^2(\Delta_m + \Delta_a + \Delta_F)^2]}. \\
&\quad\quad\quad\quad\quad\quad\quad\quad\quad\quad\quad\quad\quad\quad (B7)
\end{aligned}
$$

The mechanical gain G is defined as

$$
G = G'/\kappa_b, \quad (B8)
$$

which is the ratio between G' and the damping rate of the mechanical mode κ_b.

APPENDIX C: EFFECT OF g_{ma}, κ_a, AND κ_m ON THE MECHANICAL GAIN AND THRESHOLD POWER

The magnon-photon coupling strength g_{ma} depends on the cavity mode volume, magnetic dipole moment, and the position of YIG sphere in the resonator, which may vary in different cavity designs. The mechanical gain G as a function of the normalized detuning Δ/ω_b with smaller magnon-photon coupling strength $g_{ma}/\omega_b = 0.25$ is shown in Fig. 7(a). Compared to the larger g_{ma} case in Fig. 3(b), smaller magnon-photon coupling strength results in smaller mechanical gain [see Fig. 7(a)]. In addition, a larger pump power is required for the smaller g_{ma} case. However, the nonreciprocal phonon laser can still be obtained, as shown in Fig. 7(b).

The mechanical gain G as a function of the normalized detuning Δ/ω_b with different decay rates of photon mode κ_a is shown in Figs. 8(a) and 8(b). A larger (smaller) mechanical gain G can be obtained with smaller (larger) κ_a as compared to the results in Fig. 3(b). Similarly, a larger mechanical gain can also be achieved with smaller κ_m [see Figs. 8(a) and 8(b)]. For the threshold power, it exhibits a nonlinear response to κ_a and a linear response to κ_m. Although the decay rates of the photon and magnon modes influence the mechanical gain and threshold power, the nonreciprocity in the phonon lasing action can still be obtained.

[1] T. H. Maiman, Nature (London) **187**, 493 (1960).

[2] J. Chen and J. B. Khurgin, IEEE J. Quantum Electron. **39**, 600 (2003).

[3] K. Vahala, M. Herrmann, S. Knünz, V. Batteiger, G. Saathoff, T. Hänsch, and T. Udem, Nat. Phys. **5**, 682 (2009).

[4] A. J. Kent, R. N. Kini, N. M. Stanton, M. Henini, B. A. Glavin, V. A. Kochelap, and T. L. Linnik, Phys. Rev. Lett. **96**, 215504 (2006).

[5] I. S. Grudinin, H. Lee, O. Painter, and K. J. Vahala, Phys. Rev. Lett. **104**, 083901 (2010).

[6] A. Ganesan, C. Do, and A. Seshia, Phys. Rev. Lett. **118**, 033903 (2017).

[7] Y. Chu, P. Kharel, W. H. Renninger, L. D. Burkhart, L. Frunzio, P. T. Rakich, and R. J. Schoelkopf, Science **358**, 199 (2017).

[8] N. Li, J. Ren, L. Wang, G. Zhang, P. Hänggi, and B. Li, Rev. Mod. Phys. **84**, 1045 (2012).

[9] Z. Shen and C. Dong, Sci. China Phys. Mech. Astron. **62**, 010331 (2018).

[10] J. B. Khurgin, Physics **3**, 16 (2010).

[11] L. J. Swenson, A. Cruciani, A. Benoit, M. Roesch, C. S. Yung, A. Bideaud, and A. Monfardini, Appl. Phys. Lett. **96**, 263511 (2010).

[12] X. L. Feng, C. J. White, A. Hajimiri, and M. L. Roukes, Nat. Nanotechnol. **3**, 342 (2008).

[13] X.-F. Li, X. Ni, L. Feng, M.-H. Lu, C. He, and Y.-F. Chen, Phys. Rev. Lett. **106**, 084301 (2011).

[14] A. V. Poshakinskiy and A. N. Poddubny, Phys. Rev. Lett. **118**, 156801 (2017).

[15] S. Kim, X. Xu, J. M. Taylor, and G. Bahl, Nat. Commun. **8**, 205 (2017).

[16] C. Coulais, D. Sounas, and A. Alù, Nature (London) **542**, 461 (2017).

[17] A. Seif, W. DeGottardi, K. Esfarjani, and M. Hafezi, Nat. Commun. **9**, 1207 (2018).

[18] Y. Wang, B. Yousefzadeh, H. Chen, H. Nassar, G. Huang, and C. Daraio, Phys. Rev. Lett. **121**, 194301 (2018).

[19] Y. Jiang, S. Maayani, T. Carmon, F. Nori, and H. Jing, Phys. Rev. Appl. **10**, 064037 (2018).

[20] X. Zhang, C.-L. Zou, L. Jiang, and H. X. Tang, Phys. Rev. Lett. **113**, 156401 (2014).

[21] C. Kittel, Phys. Rev. **73**, 155 (1948).

[22] H. Huebl, C. W. Zollitsch, J. Lotze, F. Hocke, M. Greifenstein, A. Marx, R. Gross, and S. T. B. Goennenwein, Phys. Rev. Lett. **111**, 127003 (2013).

[23] Y. Tabuchi, S. Ishino, T. Ishikawa, R. Yamazaki, K. Usami, and Y. Nakamura, Phys. Rev. Lett. **113**, 083603 (2014).

[24] M. Goryachev, W. G. Farr, D. L. Creedon, Y. Fan, M. Kostylev, and M. E. Tobar, Phys. Rev. Appl. **2**, 054002 (2014).

[25] L. Bai, M. Harder, Y. P. Chen, X. Fan, J. Q. Xiao, and C.-M. Hu, Phys. Rev. Lett. **114**, 227201 (2015).

[26] D. Zhang, X.-M. Wang, T.-F. Li, X.-Q. Luo, W. Wu, F. Nori, and J. You, npj Quantum Inf. **1**, 15014 (2015).

[27] N. Kostylev, M. Goryachev, and M. E. Tobar, Appl. Phys. Lett. **108**, 062402 (2016).

[28] X. Zhang, C.-L. Zou, L. Jiang, and H. X. Tang, Sci. Adv. **2**, e1501286 (2016).

[29] M. Aspelmeyer, T. J. Kippenberg, and F. Marquardt, Rev. Mod. Phys. **86**, 1391 (2014).

[30] W. Zhao, S.-D. Zhang, A. Miranowicz, and H. Jing, Sci. China-Phys. Mech. Astron. **63**, 224211 (2020).

[31] T. J. Kippenberg, H. Rokhsari, T. Carmon, A. Scherer, and K. J. Vahala, Phys. Rev. Lett. **95**, 033901 (2005).

[32] X. Xiao, Q. Liao, N. Zhou, W. Nie, and Y. Liu, Sci. China-Phys. Mech. Astron. **63**, 114211 (2020).

[33] R. W. Andrews, R. W. Peterson, T. P. Purdy, K. Cicak, R. W. Simmonds, C. A. Regal, and K. W. Lehnert, Nat. Phys. **10**, 321 (2014).

[34] T. Bagci, A. Simonsen, S. Schmid, L. G. Villanueva, E. Zeuthen, J. Appel, J. M. Taylor, A. Sørensen, K. Usami, A. Schliesser, and E. S. Polzik, Nature (London) **507**, 81 (2014).

[35] J. Bochmann, A. Vainsencher, D. D. Awschalom, and A. N. Cleland, Nat. Phys. **9**, 712 (2013).

[36] Z.-B. Yang, J.-S. Liu, A.-D. Zhu, H.-Y. Liu, and R.-C. Yang, Ann. Phys. (Berlin) **532**, 2000196 (2020).

[37] S. Maayani, R. Dahan, Y. Kligerman, E. Moses, A. U. Hassan, H. Jing, F. Nori, D. N. Christodoulides, and T. Carmon, Nature (London) **558**, 569 (2018).

[38] R. Huang, A. Miranowicz, J.-Q. Liao, F. Nori, and H. Jing, Phys. Rev. Lett. **121**, 153601 (2018).

[39] H. Wang, Z. Wang, J. Zhang, Ş. K. Özdemir, L. Yang, and Y.-X. Liu, Phys. Rev. A **90**, 053814 (2014).

[40] M. O. Scully and M. S. Zubairy, *Quantum Optics* (Cambridge University Press, Cambridge, 1997).

[41] M.-S. Ding, L. Zheng, and C. Li, Sci. Rep. **9**, 15723 (2019).

[42] H. Jing, S. K. Özdemir, X.-Y. Lü, J. Zhang, L. Yang, and F. Nori, Phys. Rev. Lett. **113**, 053604 (2014).

[43] Y. F. Xie, Z. Cao, B. He, and Q. Lin, Opt. Express **28**, 22580 (2020).

[44] M. Song, I. Iorsh, P. Kapitanova, E. Nenasheva, and P. Belov, Appl. Phys. Lett. **108**, 023902 (2016).